PLOS | ONE

RESEARCH ARTICLE

On the Frontline: Tracking Ocean Acidification in an Alaskan Shellfish Hatchery

Wiley Evans[1,2]*, Jeremy T. Mathis[1,2], Jacqueline Ramsay[3], Jeff Hetrick[3]

1 National Oceanic and Atmospheric Administration, Pacific Marine Environmental Laboratory, Seattle, Washington, United States of America, **2** Ocean Acidification Research Center, School of Fisheries and Ocean Sciences, University of Alaska Fairbanks, Fairbanks, Alaska, United States of America, **3** Alutiiq Pride Shellfish Hatchery, Seward, Alaska, United States of America

* wiley.evans@noaa.gov

Citation: Evans W, Mathis JT, Ramsay J, Hetrick J (2015) On the Frontline: Tracking Ocean Acidification in an Alaskan Shellfish Hatchery. PLoS ONE 10(7): e0130384. doi:10.1371/journal.pone.0130384

Academic Editor: Erik V. Thuesen, The Evergreen State College, UNITED STATES

Received: February 3, 2015

Accepted: May 20, 2015

Published: July 1, 2015

Data Availability Statement: Both the hatchery data and the TA and salinity cruise data presented in this paper are available through AOOS (http://portal.aoos.org/alaska-statewide.php#module-search?page=1&tagId=118&q=). This URL will take the reader to both datasets. In addition, the validation TA and salinity samples are included as Supporting Information (S1 Table).

Funding: This work was funded by the Alaska Ocean Observing System (AOOS) and the National Oceanic and Atmospheric Administration (NOAA) Ocean Acidification Program (OAP).

Abstract

The invasion of anthropogenic carbon dioxide (CO_2) into the ocean is shifting the marine carbonate system such that saturation states of calcium carbonate ($CaCO_3$) minerals are decreasing, and this is having a detrimental impact on early life stages of select shellfish species. The global, secular decrease in $CaCO_3$ saturation states is occurring on top of a backdrop of large natural variability in coastal settings; progressively shifting the envelope of variability and leading to longer and more frequent exposure to adverse conditions. This is a great concern in the State of Alaska, a high-latitude setting vulnerable to rapid changes in the marine carbonate system, where an emerging shellfish industry plans major growth over the coming decades. Currently, the Alutiiq Pride Shellfish Hatchery (APSH) in Seward, Alaska is the only hatchery in the state, and produces many shellfish species with early life stages known to be sensitive to low $CaCO_3$ saturation states. Here we present the first land-based OA measurements made in an Alaskan shellfish hatchery, and detail the trends in the saturation state of aragonite (Ω_{arag}), the more soluble form of $CaCO_3$, over a 10-month period in the APSH seawater supply. These data indicate the largest changes are on the seasonal time scale, with extended periods of sub-optimal Ω_{arag} levels ($\Omega_{arag} < 1.5$) in winter and autumn associated with elevated water column respiration and short-lived runoff events, respectively. The data pinpoint a 5-month window of reprieve with favorable Ω_{arag} conditions above the sub-optimal Ω_{arag} threshold, which under predicted upper-bound CO_2 emissions trajectories is estimated to close by 2040. To date, many species in production at APSH remain untested in their response to OA, and the data presented here establish the current conditions at APSH as well as provide a framework for hatchery-based measurements in Alaska. The current and expected conditions seen at APSH are essential to consider for this developing Alaskan industry.

Competing Interests: The authors have declared that no competing interests exist.

Introduction

A total of nearly 155 Pg (1 Pg = 10^{15} g) of carbon have been taken by the ocean due to rising atmospheric carbon dioxide (CO_2) levels that result largely from anthropogenic fossil fuel emissions [1]. Ocean CO_2 uptake increases the concentration of hydrogen ions (H^+; lowers seawater pH) while also decreasing carbonate ion (CO_3^{2-}) levels; reactions that collectively have been termed ocean acidification (OA) [2–6]. Decreasing CO_3^{2-} has the effect of reducing the saturation state of calcium carbonate ($CaCO_3$) by the equation: $\Omega_{phase} = [Ca^{2+}][CO_3^{2-}]/K_{sp}$; where Ω_{phase} is the saturation state for typically either aragonite or calcite phases of $CaCO_3$, Ca^{2+} is the calcium concentration, and K_{sp} is the phase specific solubility product. Of these reactions associated with OA, a decrease in Ω_{phase} is a critical alteration in carbonate chemistry affecting rates of calcification and shellfish growth [7, 8]. For the aragonite phase of $CaCO_3$, Ω_{arag} values where sub-lethal sensitivity first become evident for a number of bivalve larvae range between 1.2 and 2.0 [7]. At $\Omega_{arag} < 1.0$, thermodynamics dictate aragonite will actively dissolve in seawater [9]. An unfavorable condition for aragonite precipitation is a considerable stressor for early life stages of select shellfish species that can ultimately lead to mortality [7, 8]. Due to the critical nature of this carbonate system parameter in dictating shellfish production, it is imperative for aquaculture facilities to accurately track Ω_{arag} in their seawater supplies. In the State of Alaska, having this capacity is essential for an emerging shellfish industry in the midst of a shifting biogeochemical seascape [10].

Over the time scale of a year, ocean uptake of anthropogenic CO_2 results in small incremental chemical changes. On decadal time scales, these changes can shift baselines in marine carbonate chemistry with potentially significant ecosystem level impacts [11–13]. This is especially the case in high-latitude settings where anthropogenically-driven reductions in Ω_{arag} are expected to occur ahead of changing conditions in warmer locales [14, 15]. The risk associated with such wholesale biogeochemical shifts in the marine environment will potentially have far-reaching effects beyond the ecosystems themselves and the dependence of coastal communities on ocean goods and services [10, 15]. Aquaculture hatcheries have the capacity to be important contributors to food security in support of growing populations by ingesting seawater from adjacent coastal settings in order to produce marketable marine species. As such, hatcheries are on the frontline both in terms of being one of the first industries impacted by OA [8, 11, 15, 16] and in their need to track and cope with the changing ocean biogeochemical conditions. It is important to note that in vulnerable coastal settings, secular changes in CO_2 are occurring in conjunction with large, in many cases understudied, carbonate system variability; demonstrated, for instance, by data collected on the United States (U.S.) west coast (Oregon) continental shelf over multiple years [17]. As shown by Harris et al. [17], large carbonate system variability does not diminish the importance of an increasing trend. Effectively, the gradual human-induced changes in Ω_{arag} shift the envelope of variability such that organisms experience more adverse conditions longer and more often than they would otherwise [17–19].

Pacific oyster, *Crassostrea gigas*, is a cultured species that has been described as a "canary in the coalmine" for being an organism highly impacted by reduced Ω_{arag} levels in the coastal zone [8, 16, 20]. Pacific oyster production failures in U.S. Pacific Northwest (PNW) shellfish hatcheries between 2005 and 2009 resulted from the ingestion of low- Ω_{arag}, high-pCO_2 water, which is naturally upwelled along the coast, into shore-side hatchery facilities. As detailed by Waldbusser et al. [21], adverse Ω_{arag} conditions dually impact larval *Crassostrea gigas* during D-hinge (prodissoconch I) shell formation by: (1) exposing calcification surfaces until completion of the D-hinge shell, and (2) increasing kinetic demands that then impacts the energy budget already limited by endogenous resources. The combination of these factors explains the sensitivity to $\Omega_{arag} > 1$ when aragonite is thermodynamically favored to precipitate. The

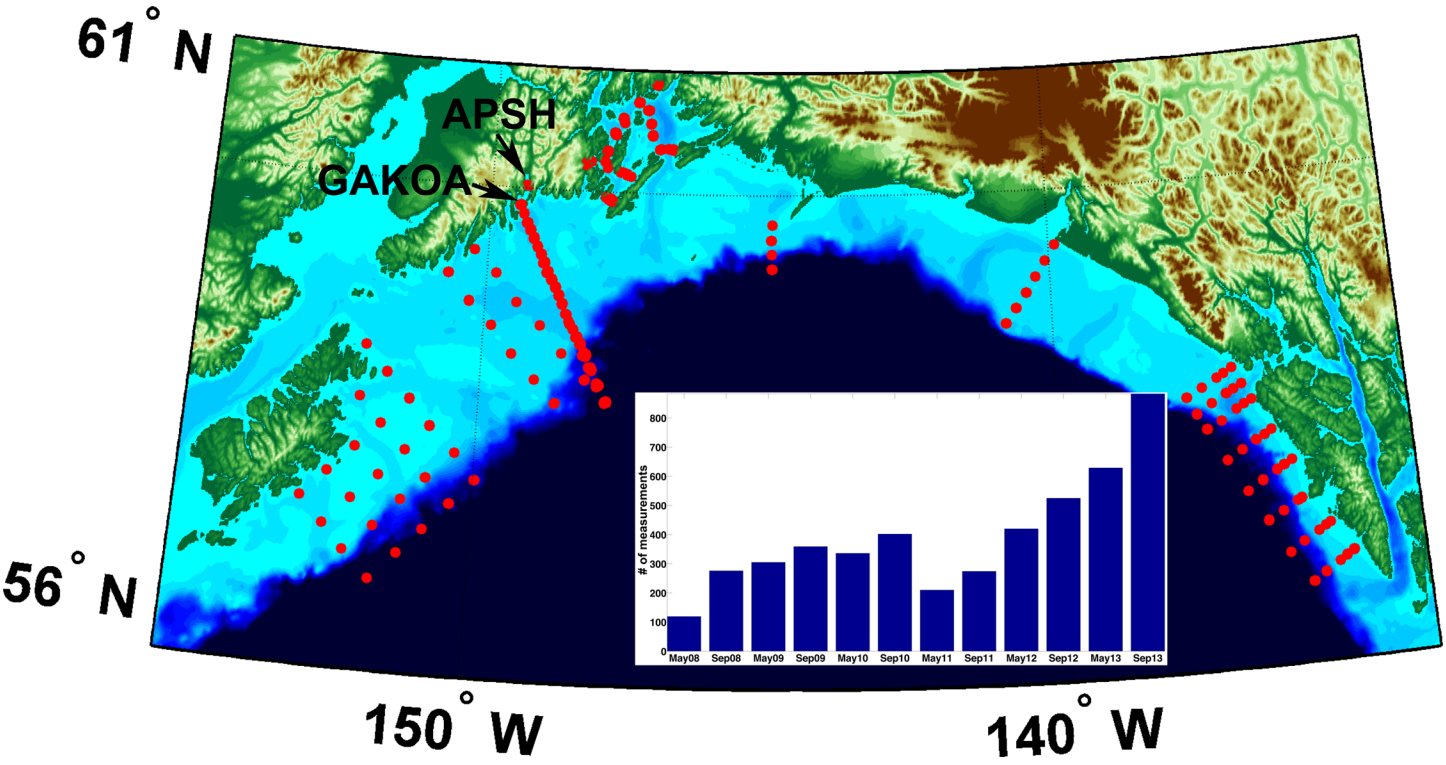

Fig 1. Map showing the location of Alutiiq Pride Shellfish Hatchery (APSH) in Resurrection Bay, the position of the Gulf of Alaska OA (GAKOA) mooring at the mouth of Resurrection Bay. Red dots are locations of discrete total alkalinity (TA) and salinity measurements, with the number of measurements made during cruises in May and September from 2008 through 2013 shown in the insert.

doi:10.1371/journal.pone.0130384.g001

additional anthropogenic CO_2 signal in upwelled water along the PNW is small relative to natural CO_2 levels in upwelling source waters [22], however large enough to alter the natural envelop of variability in these systems and impart a significant stress that resulted in a near collapse in a $270 Million industry for the State of Washington [23]. The hatchery production failures served as a vital catalyst in two ways [16]: (1) by unifying stakeholders and scientists in establishing robust monitoring techniques to track Ω_{arag} in hatchery intake water [8], and (2) by instigating state and federal government action to fund scientific activities needed to catalog trends in coastal manifestations of OA along with their impacts on marine ecosystems and the economies they support. To this end, data are presently streaming in near real-time from a number hatchery facilities along the Pacific coast of North America [24], and guidelines have been developed to aid stakeholders in making OA related land-based measurements [25].

In this contribution, we report on land-based determinations of Ω_{arag} from seawater entering an Alaskan hatchery facility in the northern Gulf of Alaska (GOA): the Alutiiq Pride Shellfish Hatchery (APSH) [26]. APSH is located in Seward, Alaska on the shore of Resurrection Bay (Fig 1) and is currently the only shellfish hatchery in the state. This is expected to change in the near future, as the Alaska Fisheries Development Foundation, Inc. currently seeks to pass an Alaska Mariculture Initiative with the aim of growing the industry to a $1 billion level in 30 years [27]. APSH is the primary producer of Blue and Red Alaskan King crab, *Paralithodes platypus* and *Paralithodes camtschaticus*, respectively. The latter crab species has been shown to be sensitive to low Ω_{arag} levels [28]. APSH also produces other animals that have either previously shown sensitivity to reduced Ω_{arag} (i.e. Pacific oyster [7, 8]) or are believed to be vulnerable during early life stages (*Panopea generosa*, *Crassadoma gigantea*, *Leukoma*

staminea). Prior to the data presented here, it was unclear whether APSH had been experiencing threatening levels of Ω_{arag} in their seawater supply. APSH is unique owing to its close proximity to an area of intense OA-related sampling from central Resurrection Bay to over the adjacent continental shelf [29]. Full water column measurements have been made in this area every May and September since 2008, and the GOA OA (GAKOA) mooring has been in place at the mouth of Resurrection Bay since 2011(Fig 1) [30]. Using high-speed measurements of the seawater entering the hatchery and a compiled dataset from the adjacent coastal ocean, trends in Ω_{arag} were resolved over a 10-month period and projections were made for the changing conditions at this integral site for the state of Alaska's growing shellfish industry.

Materials and Methods

From October 5, 2013 to August 5, 2014, temperature, salinity and CO_2 partial pressure (pCO_2) data were collected from the seawater supply flowing into APSH. This seawater supply was provided to the hatchery by the University of Alaska D. W. Hood Laboratory at the Seward Marine Center [31]. Untreated seawater was pumped to the facilities from an intake pipe extending to 75 m depth and 91 m from the laboratory into Resurrection Bay. Two seawater pumps provided flow at ~200 gallons per minute (gpm), and a tangential split off the main supply line provided seawater at ~1 gpm to the hydrographic and chemical sensors positioned in the preparation room of the D.W. Hood Laboratory. Temperature and salinity (calculated from conductivity) were measured with a Sea-Bird Electronics SBE 45 MicroTSG thermosalinograph [32], with salinity reported in this paper using the Practical Salinity Scale (PSS-78, dimensionless).

Seawater pCO_2 data were calculated from corrected measurements of CO_2 mixing ratio (xCO_2) made using a Sunburst Sensors SuperCO$_2$ System [33] following protocols recommended by Pierrot et al. [34] with the system theory and calculations described in detail elsewhere [35–38]. Seawater continuously flowed first through the thermosalinograph and then through two (primary and secondary) showerhead equilibrators [34, 39]. The primary showerhead equilibrator supplied equilibrated carrier gas (marine air) to a non-dispersive infrared gas analyzer (LI-COR LI840A CO_2/H_2O) housed within the SuperCO$_2$ system's electronics box at a rate of ~50 ml min^{-1}. Unaltered marine air was drawn from 0.25 inch polyethylene tubing that connected a vented water trap positioned outside of the D.W. Hood Laboratory to the secondary equilibrator. Marine air was pre-equilibrated in the secondary equilibrator, and then plumbed to the primary equilibrator as a make-up air supply to replace equilibrated carrier gas provided to the LI-COR. Pressure and temperature were continuously measured in the primary equilibrator using a Honeywell ASCX Microstructure Pressure Sensor and a Minco Fast Response RTD, respectively. Equilibrated carrier gas, three standard gases of known mixing ratio (148, 448 and 748 ppm; Scott-Marin, Inc.), and unaltered marine air were all plumbed to provide gas flow to the SuperCO$_2$ system's electronics box. The SuperCO$_2$ system was controlled using National Instruments LabVIEW software run on an HP laptop computer. The software controls data acquisition from the thermosalinograph, the pressure and temperature sensors, and the LI-COR; while also controlling Valco Instruments Co. Inc. (VICI) multi-port actuators that cycle between the gas streams plumbed to the electronics box. None of the gas streams were dried prior to analysis, and all measurements were made at 0.5 Hz. The prescribed measurement scheme controlled by the software was to supply equilibrated carrier gas from the primary equilibrator to the LI-COR continuously for 240 minutes, then cycle the actuators to consecutively allow the three standard gas streams and unaltered marine air to be measured for 90 s at 100 ml min^{-1} before returning to sample the carrier gas equilibrated with seawater xCO_2. From each sequence of standard gas measurements, the final 20 s of data in the

90 s interval before the actuator changed position were used to construct calibration functions that were then interpolated in time between standard gas sequences. These functions were then used to calibrate the xCO_2 measurements of seawater equilibrated carrier gas, with an adjustment on the order of 1%. Atmospheric xCO_2 measurements made by the SuperCO_2 system were not used in this analysis, as these data do not enter in to calculations of Ω_{arag}. Annual mean atmospheric pCO_2 was calculated from the well-resolved data collected on the GAKOA mooring. This annual mean atmospheric pCO_2 value was then used in anthropogenic CO_2 calculations. Corrected seawater xCO_2 was subsequently adjusted for under-pressurization in the primary showerhead equilibrator using the ratio of equilibrator to vented LI-COR cell pressure, and then converted to pCO_2 using atmospheric pressure measured by the LI-COR. The 2-s seawater pCO_2, temperature and salinity data were quality controlled, and then bin-averaged in 5-min interval bins.

Taking advantage of the expansive and growing dataset of paired total alkalinity (TA) and salinity measurements made throughout the northern GOA coastal ocean (Fig 1; [29]), these data were compiled and used to construct a TA–salinity relationship. The compiled data were collected as part of the growing suite of carbonate system and hydrographic measurements made from oceanographic cruises that have occurred every May and September since 2008. Briefly, seawater samples were collected at specific stations and depths using a rosette equipped with 5-l Niskin bottles and a Sea-Bird Electronics 911Plus conductivity-temperature-depth (CTD) profiler. Seawater was drawn from Niskin bottles into clean 250 ml Pyrex glass reagent bottles using established sampling techniques [40], and treated with 200 μl of saturated $HgCl_2$ solution to halt biological activity in the samples. TA was measured in the fixed seawater samples at the University of Alaska Fairbanks (UAF) Ocean Acidification Research Center (OARC) using a VINDTA 3C [41]. Seawater certified reference materials (provided by A. G. Dickson, Scripps Institute of Oceanography) were analyzed before samples were processed to ensure measurements were accurate to within 0.1% (2 μmol kg^{-1}). A robust linear regression was computed between the TA and salinity data using MathWorks MATLAB software. A small number of TA validation measurements (n = 23) were collected at APSH to verify the credibility of this linear relationship (S1 Table). 5-min binned seawater pCO_2 data, TA derived using the TA–salinity relationship, temperature and salinity were input into a customized MathWorks MATLAB version of CO2SYS [42] for carbonate system calculations. pH on the total hydrogen ion scale (pH_T), CO_3^{2-} and Ω_{arag} were computed using the equilibrium constants for the dissociation of carbonic acid from Millero [43]. Ca^{2+} concentrations were calculated from salinity using the relationship from Riley and Tongudai [44]. For estimating the contribution of anthropogenic CO_2 in setting Ω_{arag} variability at APSH, the mean atmospheric pCO_2 from GAKOA (398 ± 6.7 μatm) was used to calculate the sea-air difference in pCO_2 (ΔpCO_2). While the term "sub-lethal" has been used in the literature to describe the impact of Ω_{arag} levels < 1.5 on select larval shellfish species [7, 8, 15], to date, there has been no evidence of die-offs directly linked to Ω_{arag} conditions at APSH. Here, we consider Ω_{arag} values ≤ 1.5 to be sub-optimal growth conditions for many larval species produced by APSH (e.g. *Crassostrea gigas*); Ω_{arag} equal to 1.5 marks the threshold value below which increased stress and vulnerability is expected [7, 15].

Results and Discussion

Presented here are the first Ω_{arag} values from seawater entering an Alaskan shellfish hatchery, and the data indicate unique characteristics setting conditions at APSH apart from those at other hatcheries to the south along the U.S. Pacific coast within the California Current System [8]. In source waters to APSH, temperature and salinity underwent only modest changes

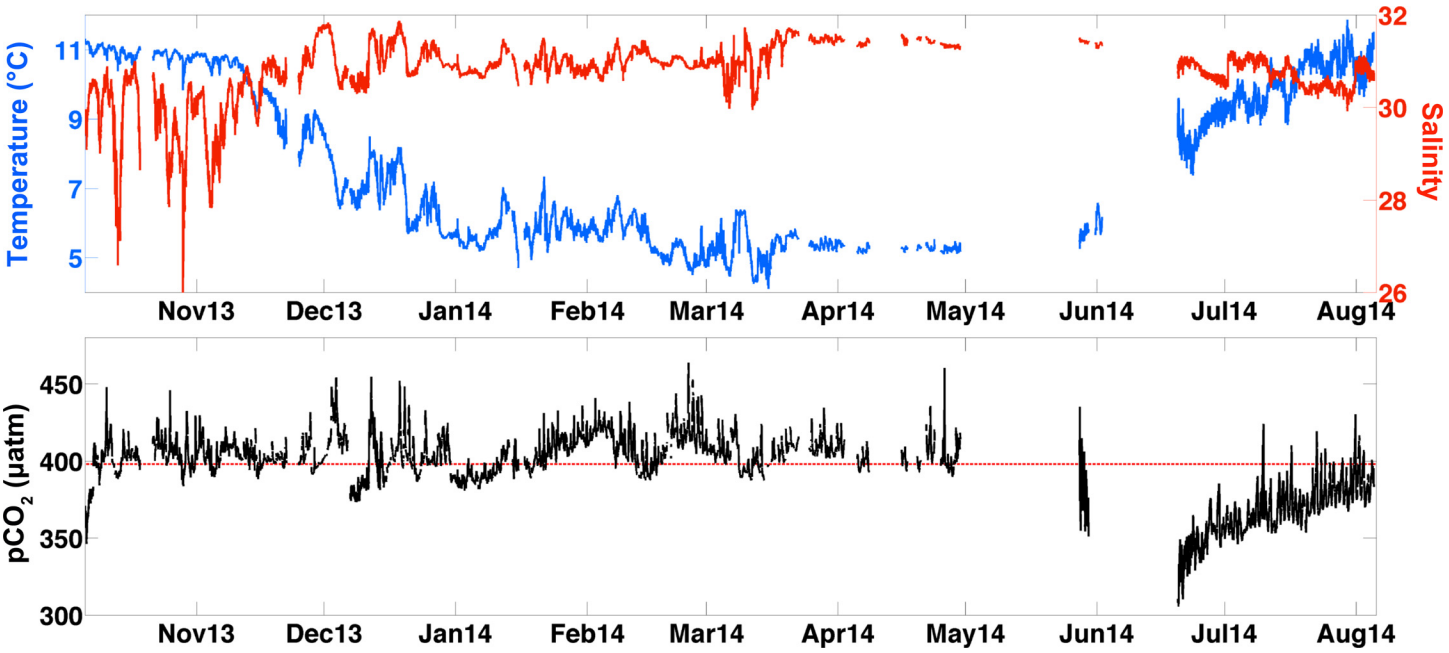

Fig 2. Ten months of data collected from intake water entering the Alutiiq Pride Shellfish Hatchery (APSH). The top panel is temperature (°C; blue) and salinity (red), and the bottom panel is seawater pCO_2 (µatm) with the red dashed horizontal line as the mean atmospheric concentration (398 ± 6.7 µatm).

doi:10.1371/journal.pone.0130384.g002

throughout the period of observation, with temperature ranging from 5 to 11°C and salinity varying between 26 and 32 (Fig 2). pCO_2 spanned 305 to 463 µatm, and was relatively confined in comparison to the dynamic range seen in surface water measured by the GAKOA buoy at the mouth of Resurrection Bay [45]. At this nearby surface site, only limited pCO_2 data above atmospheric levels have been observed to occur between February and March [30]. The most prolonged periods of high pCO_2 levels at APSH were from January to April (Fig 2). Note that record gaps in April, May and June ranged from 2 to 20 days, and were caused by either electrical power outages in Seward or technical issues associated with the SuperCO_2 system. The TA–salinity relationship built from compiled GOA data [29] was robust (Fig 3) as indicated by a high r^2 value (0.94), low root mean square error (RMSE; 17.21 µmol kg^{-1}), and close agreement with our validation samples (S1 Table). Ω_{arag}, calculated using TA from the TA–salinity relationship with the pCO_2 data, showed a smaller dynamic range of relative to the measurements made within PNW hatcheries [8], with only a 0.8 unit oscillation about the 1.5 Ω_{arag} threshold over the 10-month record (Fig 4). The largest abrupt changes in Ω_{arag} were seen during autumn runoff events (0.5 unit), whereas during July and August the near 40-µtam diurnal signal in pCO_2 (Fig 2) amounted to only 0.1 unit daily changes in Ω_{arag} (Fig 4). This small variability in Ω_{arag} is greater than the at most 0.06 unit error in the Ω_{arag} calculation estimated by propagating the RMSE value from the TA–salinity relationship with the error in the pCO_2 data (2.1 µatm; dominated by error in the LI-COR LI840A calibration functions). Short-term diurnal variability in the Alaskan hatchery is minimal in comparison to the extremes seen at the Whiskey Creak Hatchery (WCH) in Netarts Bay, Oregon where Ω_{arag} can vary by more than a whole unit over a day [8]. Ω_{arag} varies more on seasonal time scales at APSH, with highest values in July and August and low sub-optimal levels persisting from January to April. October through December is a transition period to the prolonged sub-optimal conditions in winter, which is punctuated by abrupt short-lived decreases in Ω_{arag}. Assuming that May and June also are transition months to the high summer Ω_{arag} levels, and that conditions in September are

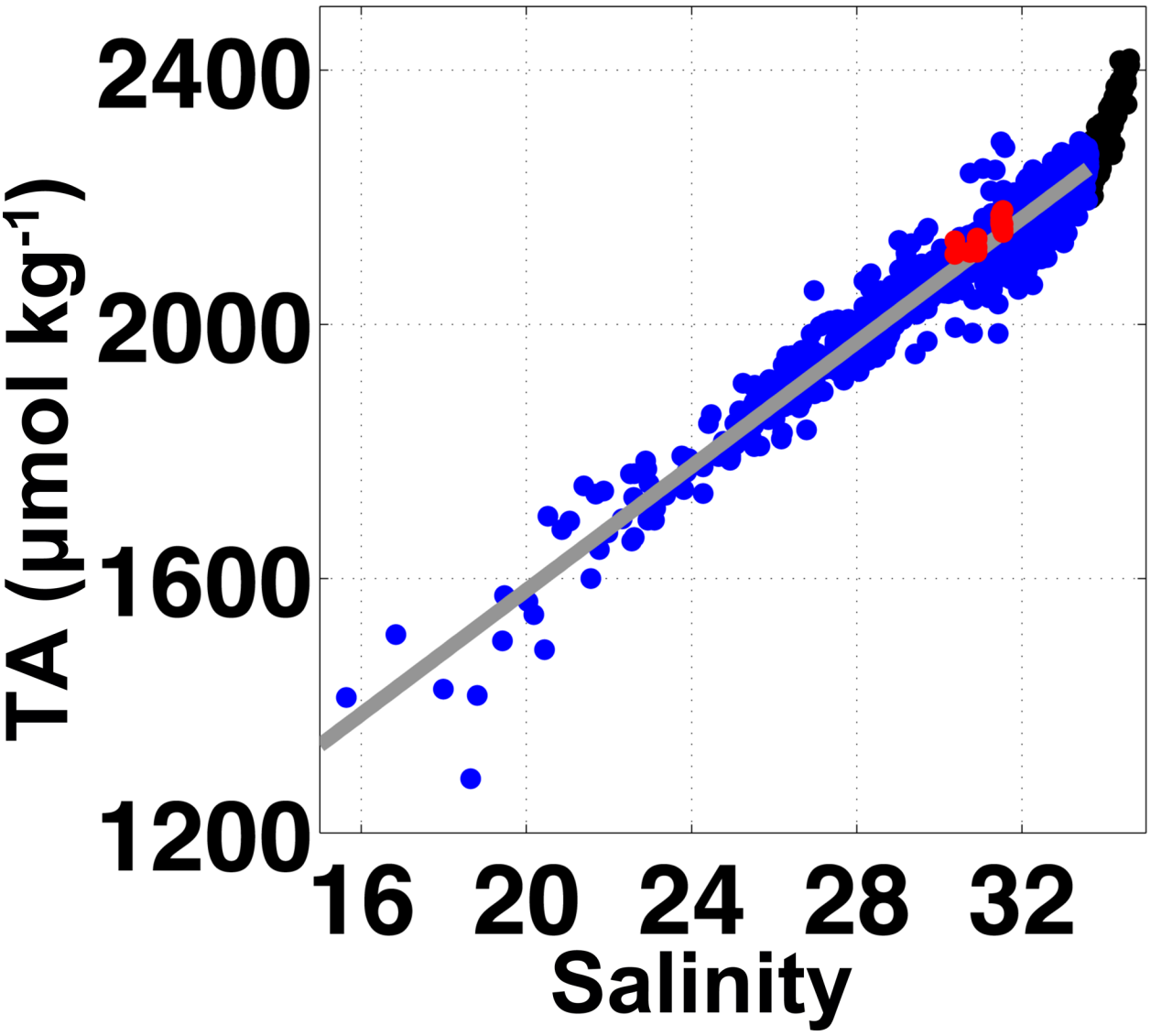

Fig 3. Relationship between total alkalinity (TA; µmol kg^{-1}) and salinity in the northern Gulf of Alaska calculated using the data described in Fig 1. The linear fit (gray line) for these data is: TA = 48.7709*S + 606.23 µmol kg^{-1} (r^2 = 0.94, root mean square error = 17.21 µmol kg^{-1}). This fit was calculated using the MathWorks MATLAB robust linear regression algorithm with only salinity data < 33.6 (blue dots). Measurements above this salinity range are deep samples collected over the outer continental shelf that have a steeper TA-salinity relationship (black dots). Twenty-three validation TA measurements (S1 Table) were made and are shown here as red dots.

doi:10.1371/journal.pone.0130384.g003

similar to those of August, this implies a 5-month window (May through September) of favorable Ω_{arag} conditions at APSH. During these 5 months, prolonged Ω_{arag} levels above the sub-optimal 1.5 Ω_{arag} threshold should alleviate this as a stressor for larval shellfish production, whereas during the other months of the year this may not be the case.

Over the 10-month period, pH_T ranged from 7.96 to 8.13 and averaged 8.03 ± 0.02. Average Ω_{arag} was near the sub-optimal threshold at 1.55 ± 0.15, with levels varying from 1.2 to 2.0. pH_T and Ω_{arag} closely tracked each other for only 6 of the 10 months of observations (Fig 4). From January to June, pH_T and Ω_{arag} were tightly coupled, with Ω_{arag} largely near or below the 1.5 Ω_{arag} threshold. pH_T and Ω_{arag} became decoupled in July, August, October and November, with pH_T depressed while Ω_{arag} persisted above the sub-optimal Ω_{arag} threshold, except during

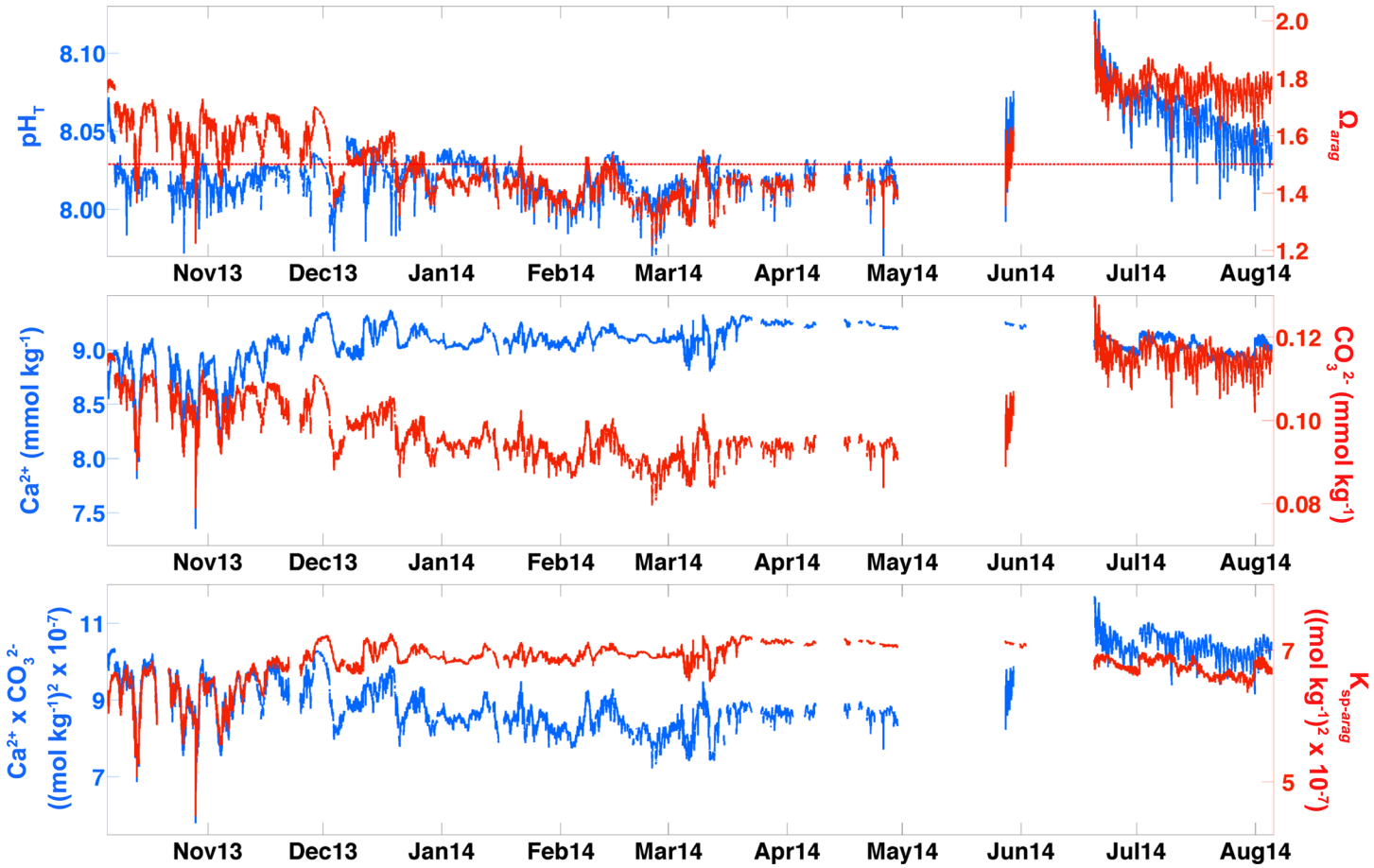

Fig 4. Top panel is pH on the total hydrogen ion scale (pH_T) and the saturation state of the aragonite phase of $CaCO_3$ (Ω_{arag}). The dashed red line is the sub-optimal 1.5 Ω_{arag} threshold. Subsequent panels are a decomposition of Ω_{arag} components: middle panel is calcium (Ca^{2+}) and carbonate (CO_3^{2-}) concentrations (mmol kg^{-1}), and bottom panel is Ca^{2+} x CO_3^{2-} ((mol $kg^{-1})^2$ x 10^{-7}) and the solubility product for aragonite ($K_{sp\text{-}arag}$; (mol $kg^{-1})^2$ x 10^{-7}).

doi:10.1371/journal.pone.0130384.g004

short-lived periods of abrupt decreases in Ω_{arag}. Maximal error in the pH_T calculations estimated by propagating pCO_2 and TA–salinity errors was 0.01 units, well below the 0.07 unit drop in pH_T during the pH_T– Ω_{arag}. The pH_T and Ω_{arag} decoupling was opposite in direction to what was observed in surface water impacted by glacial melt within nearby Prince William Sound [46], and highlights the absolute requirement to track two concurrent carbonate system parameters in order to constrain the carbonate system in coastal settings [8, 25, 47]. In this case, the decoupling was entirely temperature driven. As eloquently described by Takahashi et al. [48], the equilibrium constants for the dissociation of carbonic acid, and the $K_{sp\text{-}arag}$, are temperature and salinity dependent, with the second equilibrium constant for the dissociation of carbonic acid increasing 1.5x faster with increasing temperature than the first. This inequality in the temperature response between the two equilibrium constants drives an adjustment within the carbonate system to increase carbonic acid and CO_3^{2-} while decreasing bicarbonate ion in order to maintain charge and mass balances. Carbonic acid equals the product of CO_2 solubility and pCO_2, and the required increase in pCO_2 drives an increase in H^+ lowering pH_T. In addition to the increase in CO_3^{2-} caused by the temperature-driven shift within the carbonate system, $K_{sp\text{-}arag}$ decreases with increasing temperature and the sum of these two effects raises Ω_{arag} levels. For the months of July, August, October and November at APSH, utilizing pH alone as an indication of Ω_{arag} would produce misleading and inaccurate results.

Using output Ca^{2+}, CO_3^{2-} and $K_{sp\text{-}arag}$ data from CO2SYS, the Ω_{arag} record was decomposed into its constituents in order to pinpoint the drivers of sub-optimal Ω_{arag} levels that occurred during months outside of the window of favorable Ω_{arag} conditions (Fig 4). Ca^{2+} in the seawater supply to the hatchery ranged between 7.5 and 9.5 mmol kg^{-1}, dropping to lowest values only during brief periods when low salinity surface water was mixed vertically to the depth of the intake in October and November (Figs 2 and 4). CO_3^{2-} levels vary over a narrower range, between 0.08 and 0.13 mmol kg^{-1}, and were highest during the period of sustained low pCO_2 and warm water temperatures during July and August (Figs 2 and 4). The dynamic range of CO_3^{2-}, 51 μmol kg^{-1}, was 13x the error of 3.9 μmol kg^{-1} calculating by propagating pCO_2 and TA–salinity errors. During winter months, Ca^{2+} and $K_{sp\text{-}arag}$ were largely stable and near 9 mmol kg^{-1} and 7 (mol $kg^{-1})^2$ x 10^{-7}, respectively. The decline in Ω_{arag} over this period resulted from the steady decrease in CO_3^{2-} to a minimum in February and March (Fig 4), consistent with the period of sustained pCO_2 above atmospheric levels (Fig 2) and indicating a respiration-driven depression in Ω_{arag}. During October and November, CO_3^{2-} decreases abruptly (Fig 4) along with short-lived increases in pCO_2 above atmospheric levels (Fig 2). During this time, CO_3^{2-}, Ca^{2+} and $K_{sp\text{-}arag}$ all decrease precipitously during the episodic low salinity events (Figs 2 and 4). Low Ω_{arag} conditions during these autumn months are triggered by runoff events and match the intensity but not the length of exposure of the respiration-driven decline in Ω_{arag} seen in winter (Fig 4). In temperature-salinity space, the two differing water masses responsibly for these trends in Ω_{arag} become readily apparent, and this provides a framework for avoidance of sub-optimal Ω_{arag} levels (Fig 5). Temperature-salinity data collected over the 10-month period show a two-pronged distribution, with sub-optimal Ω_{arag} levels seen in water masses with the lowest salinities (<29) and coldest temperatures (< 7°C). Both of these water mass types have high pCO_2 with respect to the atmosphere (Fig 2), and these temperature–salinity–pCO_2 characteristics set up a diagnostic for APSH to respond to adverse Ω_{arag} conditions in the absence of real-time Ω_{arag} calculations.

The 5-month window of favorable Ω_{arag} conditions at APSH will shrink in the future under the continued increase in anthropogenic CO_2 emissions. Using the approach of Harris et al. [17], we can subtract the anthropogenic CO_2 signal from the APSH pCO_2 data by making the assumptions that the sea-air CO_2 disequilibrium is roughly constant as are the processes shaping the distributions of TA, salinity and temperature. In this same way, we can also add additional anthropogenic CO_2 to pinpoint when the window of favorable growth conditions may close. Target atmospheric pCO_2 levels were added to APSH ΔpCO_2 data computed using the mean atmospheric pCO_2 from GAKOA (Figs 1 and 2) with the result being an adjusted seawater pCO_2 record. Ω_{arag} at the target atmospheric pCO_2 levels were calculated with CO2SYS using the adjusted seawater pCO_2, TA, salinity and temperature data. Under a pre-industrial atmospheric pCO_2 level (pCO_2 = 280 μatm), the window for favorable Ω_{arag} conditions is open the entire year (Fig 6); none of the estimated Ω_{arag} levels fell below the 1.5 Ω_{arag} threshold. Note that the average difference between total CO_2 calculated using both unadjusted seawater pCO_2 and adjusted seawater pCO_2 to a pre-industrial atmosphere with TA, salinity and temperature data was 52.4 μmol kg^{-1}. This was in close agreement with an independent estimate of the total CO_2 addition from anthropogenic CO_2 uptake on density surfaces < 26.9 kg m^{-3} in the North Pacific until 2006 and scaled to 2014 using a growth rate of 1.62 μmol kg^{-1} yr^{-1} (47.96 μmol kg^{-1}) [49]. Atmospheric pCO_2 concentrations were then iteratively increased beyond the mean 2014 atmospheric level to estimate when the window of favorable Ω_{arag} conditions may close. The atmospheric pCO_2 at which this occurred was 500 μatm (Fig 6). Under the Intergovernmental Panel on Climate Change (IPCC) representative concentration pathway (RCP) emissions scenario 8.5, this atmospheric pCO_2 threshold will be reached by approximately 2040 [50]. Ω_{arag} levels at APSH in 2040 would still remain above the thermodynamic

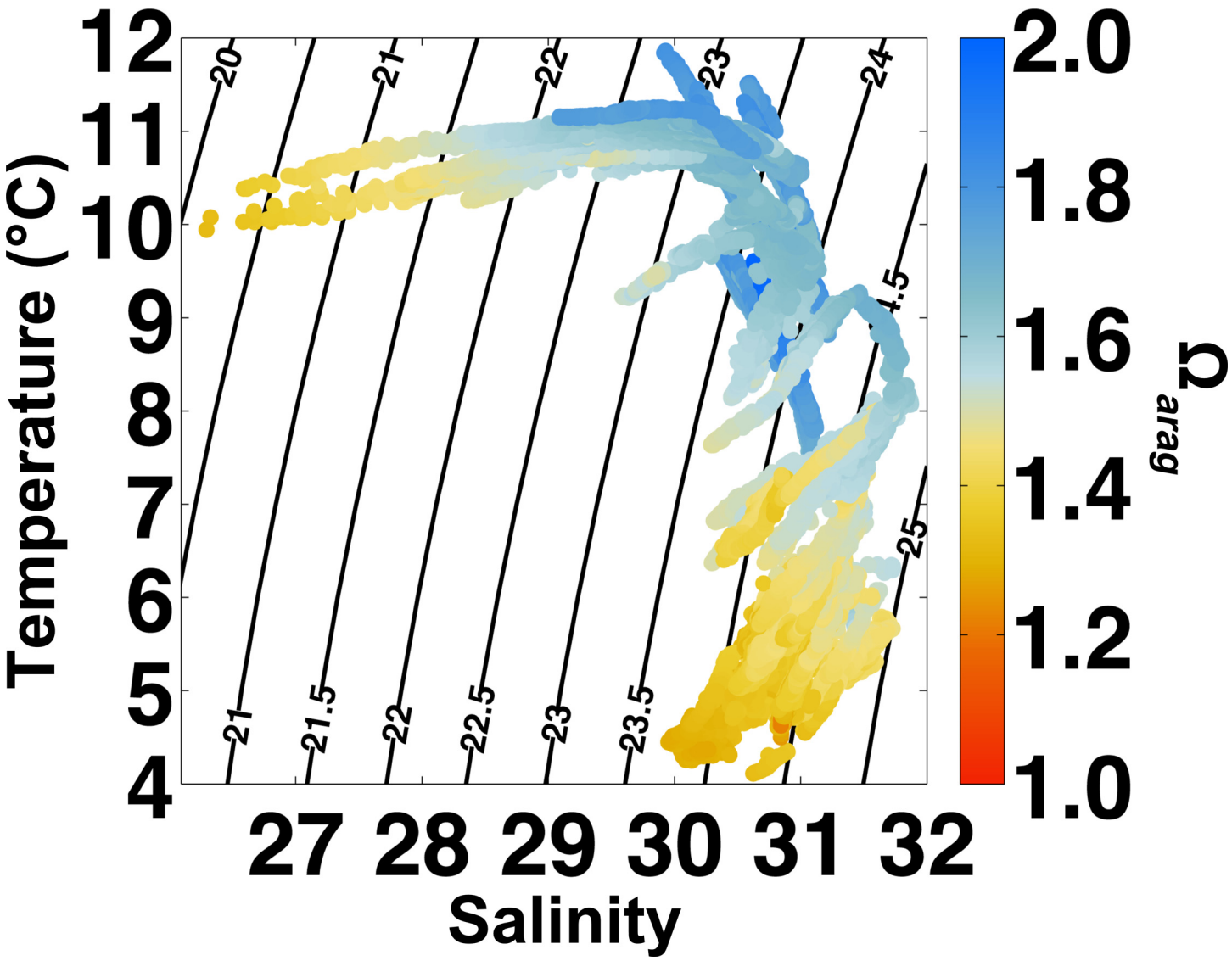

Fig 5. Temperature (°C)–salinity diagram with contours of seawater potential density anomaly (σ_t) and Ω_{arag} as colored dots. Note the two areas of sub-optimal Ω_{arag} (Ω_{arag} < 1.5; warm colors) at the lowest salinities (<29) and coldest temperatures (< 7°C).

doi:10.1371/journal.pone.0130384.g005

threshold for aragonite dissolution (Ω_{arag} = 1; Fig 6), but clearly seawater manipulation strategies will need to be in place by this time in order to facilitate conditions favorable for larval shellfish production.

Conclusions

The window of favorable Ω_{arag} conditions in source waters to APSH is gradually closing, and this biogeochemical shift is consistent across the coastal Gulf of Alaska [10, 15, 51]. In 3 decades, sub-optimal Ω_{arag} levels will be a constant condition for this premier Alaskan hatchery (Fig 6). Manipulation strategies will need to be invoked to alter the carbonate chemistry of the seawater supply, or alternatively draw seawater from a shallower depth at the risk of experiencing a higher frequency of low Ω_{arag} runoff events. Inherently this implies a decreased volume in the water column of Resurrection Bay containing Ω_{arag} above the sub-optimal threshold, and

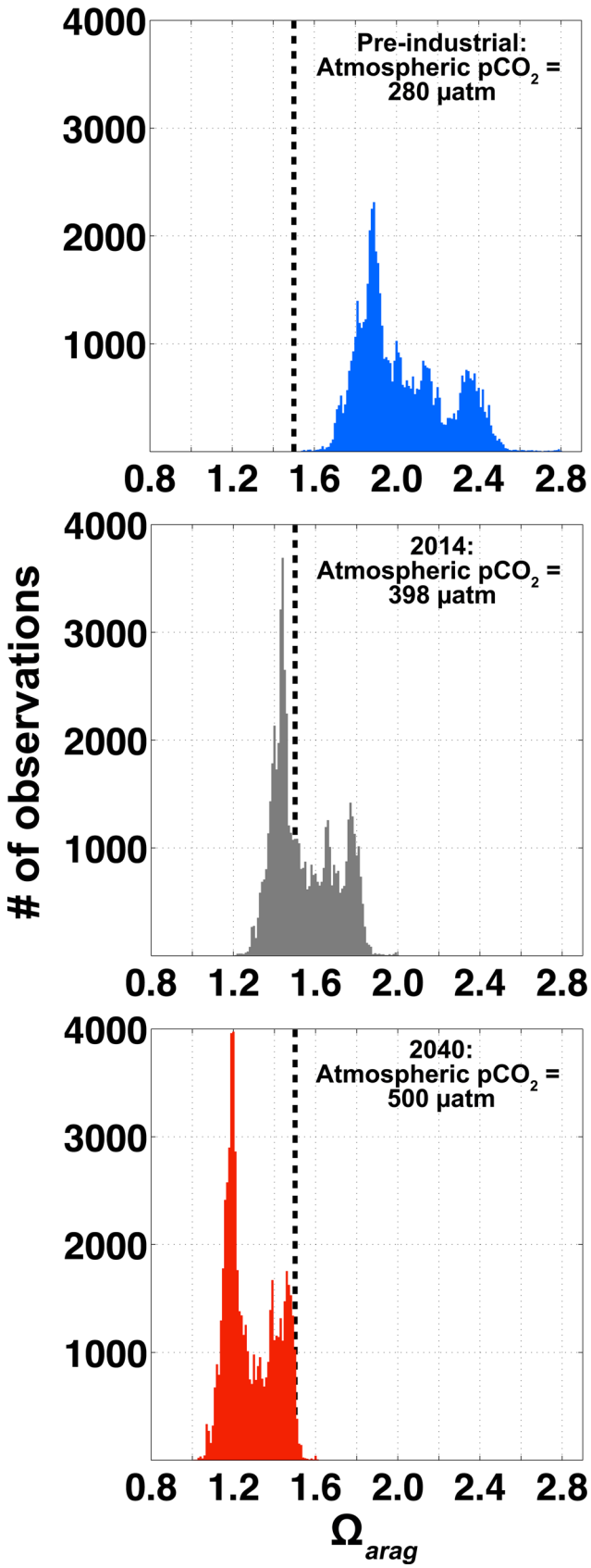
Pre-industrial:
Atmospheric pCO2 =
280 µatm
2014:
Atmospheric pCO2 =
398 µatm
2040:
Atmospheric pCO2 =
500 µatm
# of observations
4000
3000
2000
1000
0.8
1.2
1.6
2.0
2.4
2.8
Ωarag

Fig 6. Bar graphs showing histograms of Ω_{arag} observations at APSH. The center panel is the data shown in Fig 4 with 2014 atmospheric pCO_2 levels (398 μatm; gray). Top and bottom panels are Ω_{arag} computed using total CO_2 (TCO_2) adjusted to atmospheric pCO_2 levels of 280 (blue) and 500 (red) μatm, respectively, following the approach of Harris et al. [17] by assuming sea-air CO_2 disequilibria and the processes that determine TA, temperature and salinity variability are constant in time. The vertical dashed black line in all panels is the sub-optimal 1.5 Ω_{arag} threshold where some early life stages of marine bivalves become stressed [7, 8]. An atmospheric pCO_2 of 500 is expected by 2040 if the IPCC AR5 RCP 8.5 emissions trajectory is realized.

doi:10.1371/journal.pone.0130384.g006

this has implications for natural populations of vulnerable shellfish species in the region. A limited number of studies examining biological impacts due to shifting carbonate chemistry in Alaskan coastal waters exist [28], and additional studies are essential for detailing the severity of these changes for natural and cultured assemblages. Most of the species currently in production at APSH remain untested in their response to OA. The data presented here establish the current conditions experienced by APSH, and provide a framework for hatchery-based measurements in Alaska. For Alaska's growing shellfish aquaculture industry to reach its target growth and be successful in the shifting biogeochemical climate of the coastal ocean, the implementation of robust measures for tracking Ω_{arag} are key, as are strong partnerships between stakeholders and scientists. State and federal government provision of OA-related scientific research that directly supports stakeholders such as the Alaskan shellfish industry is an excellent model for simultaneously backing industry while progressing scientific initiatives.

Supporting Information

S1 Table. Validation measurements (n = 23) of temperature, salinity and total alkalinity collected in the hatchery during the 10-month period of observation.
(EPS)

Acknowledgments

We would like to thank Phyllis Shoemaker, Linda Lasota and Jennifer Elhard from the University of Alaska Seward Marine Center for their support throughout this project. We thank the Alaska Ocean Observing System (AOOS) and the National Oceanic and Atmospheric Administration (NOAA) Ocean Acidification Program (OAP) for funding this research. Both the hatchery data and the TA and salinity cruise data presented in this manuscript are available through AOOS (http://portal.aoos.org/alaska-statewide.php#module-search?page=1&tagId=118&q=). This is PMEL contribution number 4285.

Author Contributions

Conceived and designed the experiments: WE JTM JH. Performed the experiments: WE JR JH. Analyzed the data: WE. Contributed reagents/materials/analysis tools: WE JTM. Wrote the paper: WE JTM JR JH. Oversaw routine operation and maintenance of the sensors used to collect data for this project: JR. Provided the facility in which WE and JTM installed their sensors: JH.

References

1. Feely RA, Wanninkhof R, Sabine CL, Mathis JT, Takahashi T, Khatiwala S. Global ocean carbon cycle. In: Blunden J, Arndt DS, editors. State of the Climate in 2013. 95: Bulletin of the American Meteorological Society; 2014. p. 73–8.
2. Doney SC, Fabry VJ, Feely RA, Kleypas JA. Ocean Acidification: The Other CO_2 Problem. Annual Review of Marine Science. 2009; 1:169–92. PMID: 21141034

3. Raven J, Caldeira K, Elderfield H, Hoegh-Guldberg O, Liss PS, Riebesell U, et al. Ocean acidification due to increasing atmospheric carbon dioxide. The Royal Society, 2005.
4. Caldeira K, Wickett ME. Anthropogenic carbon and ocean pH. Nature. 2003; 425:365. PMID: 14508477
5. Orr JC, Fabry VJ, Aumont O, Bopp L, Doney SC, Feely RA, et al. Anthropogenic ocean acidification over the twenty-first century and its impact on calcifying organisms. Nature. 2005; 437:681–6. PMID: 16193043
6. Feely RA, Sabine CL, Lee K, Berelson W, Kleypas J, Fabry VJ, et al. Impact of Anthropogenic CO_2 on the $CaCO_3$ System in the Oceans. Science. 2004; 305:362–6. PMID: 15256664
7. Waldbusser GG, Hales B, Langdon CJ, Haley BA, Schrader P, Brunner EL, et al. Saturation-state sensitivity of marine bivalve larvae to ocean acidification. Nature Climate Change. 2014. doi: 10.1038/nclimate2479
8. Barton A, Hales B, Waldbusser G, Langdon C, Feely RA. The Pacific oyster, *Crassostrea gigas*, shows negative correlation to naturally elevated carbon dioxide levels: Implications for near-term ocean acidification effects. Limnology and Oceanography. 2012; 57(3):698–710.
9. Millero FJ. The Marine Inorganic Carbon Cycle. Chemical Reviews. 2007; 107:308–41. PMID: 17300138
10. Mathis JT, Cooley SR, Lucey N, Colt S, Ekstrom J, Hurst T, et al. Ocean acidification risk assessment for Alaska's fishery sector. Progress in Oceanography. 2014. doi: 10.1016/j.pocean.2014.07.001
11. Feely RA, Klinger T, Newton JA, Chadset M. Scientific Summary of Ocean Acidification in Washington State Marine Waters. 2012.
12. Fabry VJ, Seibel BA, Feely RA, Orr JC. Impacts of ocean acidification on marine fauna and ecosystem processes. ICES Journal of Marine Science. 2008; 65:414–32.
13. Bednarsek N, Feely RA, Reum JC, Peterson B, Menkel J, Alin SR, et al. Limacina helicina shell dissolution as an indicator of declining habitat suitability owing to ocean acidification in the California Current Ecosystem. Proceedings Biological sciences / The Royal Society. 2014; 281(1785):20140123. doi: 10.1098/rspb.2014.0123 PMID: 24789895; PubMed Central PMCID: PMC4024287.
14. Fabry VJ, McClintock JB, Mathis JT, Grebmeier JM. Ocean Acidification at High Latitudes: The Bellwether. Oceanography. 2009; 22(4):160–71.
15. Ekstrom JA, Suatoni L, Cooley SR, Pendleton LH, Waldbusser GG, Cinner JE, et al. Vulnerability and adaptation of US shellfisheries to ocean acidification. Nature Climate Change. 2015; 5(3):207–14. doi: 10.1038/nclimate2508
16. Kelly RP, Cooley SR, Klinger T. Narratives can motivate environmental action: the Whiskey Creek ocean acidification story. Ambio. 2014; 43(5):592–9. doi: 10.1007/s13280-013-0442-2 PMID: 24081705; PubMed Central PMCID: PMC4132469.
17. Harris KE, Degrandpre MD, Hales B. Aragonite saturation state dynamics in a coastal upwelling zone. Geophysical Research Letters. 2013; 40:2720–5. doi: 10.1002/grl.50460
18. Gruber N, Hauri C, Lachkar Z, Loher D, Frolicher TL, Plattner GK. Rapid progression of ocean acidification in the California Current System. Science. 2012; 337(6091):220–3. doi: 10.1126/science.1216773 PMID: 22700658.
19. Waldbusser GG, Salisbury JE. Ocean acidification in the coastal zone from an organism's perspective: multiple system parameters, frequency domains, and habitats. Ann Rev Mar Sci. 2014; 6:221–47. doi: 10.1146/annurev-marine-121211-172238 PMID: 23987912.
20. Scigliano E. The Great Oyster Crash. OnEarth. 2011 August 17, 2011.
21. Waldbusser GG, Brunner EL, Haley BA, Hales B, Langdon CJ, Prahl FG. A developmental and energetic basis linking larval oyster shell formation to acidification sensitivity. Geophysical Research Letters. 2013; 40(10):2171–6. doi: 10.1002/grl.50449
22. Feely RA, Sabine CL, Hernandez-Ayon M, Ianson D, Hales B. Evidence for Upwelling of Corrosive "Acidified" Water onto the Continental Shelf. Science. 2008; 320(5882):1490–2. doi: 10.1126/science.1155676 PMID: 18497259
23. Adelsman H, Whitely Binder L. Ocean Acidifaction: From Knowledge to Action, Washington State's Strategic Response. Washington State Blue Ribbon Panel on Ocean Acidification. Olympia, Washington Washington Department of Ecology; 2012.
24. IOOS. IOOS Pacific Region Ocean Acidification 2015. Available: http://www.ipacoa.org.
25. McLaughlin K, Weisberg SB, Alin S, Barton A, Capson T, Dickson A, et al. Guidance Manual for Establishing a Land-Based Station for Measurement of Ocean Acidification Parameters. 2014.
26. Ramsay J. Alutiiq Pride Shellfish Hatchery on Resurrection Bay, Seward, Alaska 2015. Available: http://alutiiqpridehatchery.com.

27. AFDF. Alaska Mariculture Initiative: Grow a $1 billion industry in 30 years 2015. Available: http://www.afdf.org/alaska-mariculture-initiative-recommended-for-noaa-funds/.
28. Long WC, Swiney KM, Harris C, Page HN, Foy RJ. Effects of ocean acidification on juvenile red king crab (Paralithodes camtschaticus) and Tanner crab (Chionoecetes bairdi) growth, condition, calcification, and survival. PLoS One. 2013; 8(4):e60959. doi: 10.1371/journal.pone.0060959 PMID: 23593357; PubMed Central PMCID: PMC3617201.
29. Mathis JT, Evans W, Cross JN, Weingartner TJ, Monacci N. The Physical and Biogeochemical Controllers on Ocean Acidification in the Northern Gulf of Alaska. Journal of Geophysical Research. 2015:in preparation.
30. NOAA/PMEL. GAKOA: Gulf of Alaska Ocean Acidification Mooring (59.85°N 149.5°W) 2015. Available: http://www.pmel.noaa.gov/co2/story/GAKOA.
31. UAF. University of Alaska Fairbanks Seward Marine Center 2015. Available: https://http://www.sfos.uaf.edu/smc/.
32. SBE. Sea-Bird Electronics SBE 45 MicroTSG Thermosalinograph 2015. Available: http://www.seabird.com/sbe45-thermosalinograph.
33. Beck J. SuperCO_2 System 2015. Available: http://www.sunburstsensors.com/products/oceanographic-carbon-dioxide-sensor-benchtop-li-cor.html.
34. Pierrot D, Neill C, Sullivan K, Castle R, Wanninkhof R, Lüger H, et al. Recommendations for autonomous underway pCO_2 measureing systems and data-reduction routines. Deep-Sea Research II. 2009; 56:512–22.
35. Evans W, Hales B, Strutton PG. The seasonal cycle of surface ocean pCO_2 on the Oregon shelf. Journal of Geophysical Research. 2011; 116(C05012): doi: 10.1029/2010JC006625 PMID: 24383048
36. Hales B, Chipman D, Takahashi T. High-frequency measurements of partial pressure and total concentration of carbon dioxide in seawater using microporous hydrophobic membrane contactors. Limnology and Oceanography: Methods. 2004; 2:356–64.
37. Evans W, Hales B, Strutton PG. pCO_2 distributions and air-water CO_2 fluxes in the Columbia River estuary. Estuarine, Coastal and Shelf Science. 2013; 117: doi: 10.1016/j.ecss.2012.12.003
38. Evans W, Hales B, Strutton PG, Ianson D. Sea-air CO_2 fluxes in the western Canadian coastal ocean. Progress in Oceanography. 2012: doi: 10.1016/j.pocean.2012.01.003
39. Takahashi T. Carbon Dioxide in the Atmosphere and in Atlantic Ocean Water. Journal of Geophyiscal Research. 1961; 66(2):477–94.
40. Dickson AG, Sabine CL, Christian JR, editors. Guide to Best Practices for Ocean CO_2 Measurements: North Pacific Marine Science Organization; 2007.
41. Marianda. Total alkalinity and dissolved inorganic carbon in seawater (VINDTA 3C) 2015. Available: http://www.marianda.com/index.php?site = products&subsite = vindta3c.
42. van Heuven S, Pierrot D, Rae JWB, Lewis E, Wallace DWR. MATLAB Program Developed for CO_2 System Calculations Oak Ridge, Tennessee: Department of Energy, 2011.
43. Millero FJ. Carbonate constants for estuarine waters. Marine and Freshwater Research. 2010; 61 (2):139–42.
44. Riley JP, Tongudai M. The major cation/chlorinity ratios in seawater Chemical Geology. 1967; 2:263–9.
45. Evans W, Mathis JT. The Gulf of Alaska coastal ocean as an atmospheric CO_2 sink. Continental Shelf Research. 2013; 65:52–63.
46. Evans W, Mathis JT, Cross JN. Calcium Carbonate Corrosivity in an Alaskan Inland Sea. Biogeosciences. 2014; 11:365–79. doi: 10.5194/bg-11-365-2014
47. Cullison Gray SE, Degrandpre M, Moore TS, Martz TR, Friederich GE, Johnson KS. Applications of *in situ* pH measurements for inorganic carbon calculations. Marine Chemistry. 2011; 125:82–90.
48. Takahashi T, Sutherland SC, Chipman DW, Goddard JG, Ho C, Newberger T, et al. Climatological distributions of pH, pCO2, total CO2, alkalinity, and CaCO3 saturation in the global surface ocean, and temporal changes at selected locations. Marine Chemistry. 2014; 164:95–125. doi: 10.1016/j.marchem.2014.06.004
49. Watanabe YW, Chiba T, Tanaka T. Recent change in the oceanic uptake rate of anthropogenic carbon in the North Pacific subpolar region determined by using a carbon-13 time series. Journal of Geophysical Research. 2011; 116(C2). doi: 10.1029/2010jc006199
50. van Vuuren DP, Edmonds J, Kainuma M, Riahi K, Thomson A, Hibbard K, et al. The representative concentration pathways: an overview. Climatic Change. 2011; 109(1–2):5–31. doi: 10.1007/s10584-011-0148-z
51. Mathis JT, Cross JN, Evans W, Doney SC. Ocean Acidification in the Surface Waters of the Pacific-Arctic Boundary Regions. Oceanography. 2015:Accepted.